Catal Lett (2008) 121:241–246
DOI 10.1007/s10562-007-9322-3

CO Hydrogenation to C_2-oxygenates over Rh–Mn–Li/SiO_2 Catalyst: Effects of Support Pretreatment with $n$$C_1$–$C_5$ Alcohols

Dahao Jiang · Yunjie Ding · Zhendong Pan ·
Weimiao Chen · Hongyuan Luo

Received: 3 July 2007 / Accepted: 24 October 2007 / Published online: 7 November 2007

Abstract The effects of support pretreatment with $n$$C_1$–$C_5$ alcohols on the performance of Rh–Mn–Li/SiO_2 catalyst in the synthesis of C_2-oxygenates from syngas have been investigated by CO hydrogenation reaction, transmission electron microscopy (TEM), pulse adsorption of CO and H_2, and Fourier Transform infrared (FT-IR) spectroscopy. The catalysts prepared from the pretreated silica supports exhibited higher space time yields of C_2-oxygenates ($STY_{C2\text{-}oxy}$) and selectivities towards C_2-oxygenates ($S_{C2\text{-}oxy}$) than that prepared from the untreated silica support. The enhancement in the hydrophobicity of the pretreated silica supports would be favorable for increasing Rh dispersion and ratio of Rh^+/Rh^0 sites, therefore increasing the number of active sites, especially the active sites for CO insertion. Such variations are responsible for the improvements in the catalytic performance of the Rh–Mn–Li/SiO_2 catalyst.

Keywords $n$$C_1$–$C_5$ alcohols · Support pretreatment · Rh-based catalyst · C_2-oxygenates · CO hydrogenation

1 Introduction

As one of the alternative means for producing clean fuels and raw chemicals from non-petroleum sources, the catalytic conversion of syngas to C_2-oxygenates such as ethanol, acetaldehyde and acetic acids has attracted much attention in the past decades. So far, the Rh–Mn–Li/SiO_2 catalyst, usually prepared by the impregnation method, has been proven to be one of the most promising catalyst systems for the synthesis of C_2-oxygenates from syngas [1]. However, in order to commercialize this C_2-oxygenates synthesis process, further improvements in the performance of CO hydrogenation over the Rh–Mn–Li/SiO_2 catalyst are necessary.

Silica is one of the most extensively used catalyst supports due to its high surface area, ample porosity, and good stability. Besides the textural properties, the surface properties of the silica gel also play an important role in determining the performance of supported-metal catalysts [2–4]. Qu et al. [3] have reported that the catalytic properties of a Ag/SiO_2 catalyst for the selective oxidation of CO in excess hydrogen were enhanced by calcination of the silica support at appropriate temperatures due to a preferential removal of the H-bonded Si–OH from the silica surface, thus resulting in an improvement of the Ag dispersion. Ho et al. [4] have studied the effect of ethanol as the impregnation solvent on the properties of cobalt-silica FTS catalyst, and observed that the ethoxyl groups formed on the silica surface could lead to the formation of smaller cobalt particle. Moreover, Zhang et al. [5] have reported that pretreatment of the silica support with organic solvents could enhance remarkably the catalytic activities of Co-based catalysts for liquid phase FTS, owing to the greatly increased dispersion and the high degree of reduction of the supported cobalt component.

In the present paper, the effects of support pretreatment with $n$$C_1$–$C_5$ alcohols on the catalytic properties of an Rh–Mn–Li/SiO_2 catalyst has been investigated via CO hydrogenation reaction, TEM, pulse adsorption of CO and H_2, and FT-IR. To the best of our knowledge, this is the

D. Jiang · Y. Ding (✉) · Z. Pan · W. Chen · H. Luo
Dalian Institute of Chemical Physics,
Chinese Academy of Sciences, Dalian 116023, China
e-mail: dyj@dicp.ac.cn

D. Jiang · Z. Pan
Graduate School of the Chinese Academy of Sciences,
Beijing 100039, China

first attempt for improving the catalytic properties of Rh-based catalysts for C_2-oxygenates synthesis from syngas by means of surface modification of the silica supports.

2 Experimental

2.1 Support Pretreatment

Silica gel (BET surface area ca. 200 m^2/g, Qingdao Haiyang Chemicals Co.) was dried at 383 K for 4 h, and then used as the silica support in this study. For support pretreatment, the silica gels (2 g) were treated with 5 mL of C_1–C_5 normal alcohols by the impregnation method. The resultant silica gels were dried at 383 K for 4 h after preliminarily dried under ambient conditions.

2.2 Catalyst Preparation

The catalysts were prepared by co-impregnating the silica supports with aqueous solutions containing $RhCl_3$, $MnCl_2$, and LiCl. The impregnated catalysts were dried for ca. 5 days at room temperature and then further dried at 383 K for 4 h. The catalysts prepared from the pretreated silica supports were designated as Rh/Silica-C_xOH ($x = 1$–5); here C_xOH was normal alcohols such as methanol, ethanol, 1-prothanol, 1-buthanol, and 1-penthanol, and Silica-C_xOH was the silica supports pretreated with C_xOH. An Rh/Silica catalyst, which was prepared from the untreated silica support, was used as the reference. For all catalysts, the Rh loading was 1.5 wt% and the weight ratio of Rh:Mn:Li was 1:0.35:0.025. The $RhCl_3$ was purchased from Johnson Matthey Precious Metal Corporation. Other metal salts were purchased from No. 3 Plant of Tianjin Chemical Agents.

2.3 Catalytic Tests

CO hydrogenation reactions were carried out in a fixed-bed micro-reactor under 553 K, 5.0 MPa ($H_2/CO = 2$) and GHSV = 12,500 h^{-1}. Before the reaction, all the catalysts were in-situ activated at 623 K for 1 h in a flow of H_2. The reaction effluent passed through a condenser filled with cold deionized water, and was subsequently analyzed by an on-line Agilent 3000A Micro GC with four packed columns respectively, namely, molecule sieve, Plot Q, Al_2O_3, and OV-1, and a TCD. The produced oxygenates, captured by complete dissolution into the deionized water, were analyzed off-line by a Varian 3800 GC with an HP-FFAP capillary column and an FID, using *n*-pentanol as an internal standard.

2.4 Catalyst Characterization

Transmission electron microscopy (TEM) measurements were carried out using a Tecnai G^2 Spirit microscope operated at an accelerating voltage of 120 kV. The catalysts were reduced for 1 h in H_2 at 623 K before testing. The samples were then ultrasonically suspended in ethanol and placed onto a carbon film supported on a copper grid. The size and shape of the Rh particles were obtained by analyzing the TEM images.

Pulse adsorption of CO or H_2 was performed on a Micromeritics Autochem 2910 apparatus. About 200 mg of the catalyst sample was reduced for 1 h in flowing H_2 at 623 K, then purged by He or Ar at the same temperature for 0.5 h, and finally cooled down to 323 K. Uptake of CO or H_2 was measured by injecting 5% CO–He into the He carrier gas or 10% H_2–Ar into the Ar carrier gas in a pulsed mode.

Fourier Transform infrared (FT-IR) spectra of adsorbed CO were recorded by a BRUKER EQUINOX 55 single-beam FT-IR spectrometer. The sample was first reduced for 1 h in flowing H_2 at 623 K, followed by purging with N_2 for 30 min. When this sample was cooled to 323 K in a N_2 flow, an FT-IR spectrum (denoted as spectrum A) of the catalyst was recorded. Then, pure CO was introduced into this system for 30 min. The catalyst was then purged again with N_2 for 30 min, and spectrum B was recorded. Subtracting spectrum A from spectrum B gave a final IR spectrum. All spectra were recorded with 16 scans and the resolution was 4 cm^{-1}.

The surface properties of the untreated and pretreated silica supports were also analyzed by IR. The procedure for the IR measurements was as follows: the sample was first placed in the IR-reactor cell, and then purged with N_2 at 383 K for 3 h to eliminate moisture. When the temperature was reduced to room temperature, the IR spectrum of the sample was recorded using air as the background.

3 Results and Discussion

3.1 CO Hydrogenation Performances of the Catalysts

Performances of CO hydrogenation over the various Rh-based catalysts are presented in Table 1. The catalyst Rh/Silica showed a normal catalytic performance, as indicated by the space time yield of C_2-oxygenates ($STY_{C2\text{-}oxy}$) and the selectivity to C_2-oxygenates ($S_{C2\text{-}oxy}$) of 493.6 g/(kg-cat h) and 71.2%, respectively. The catalysts prepared from the pretreated silica supports exhibited higher $STY_{C2\text{-}oxy}$ and $S_{C2\text{-}oxy}$ than those over the Rh/Silica catalyst. Especially, the catalyst Rh/Silica-C_4OH displayed $STY_{C2\text{-}oxy}$ and $S_{C2\text{-}oxy}$ up to 630.8 g/(kg-cat h) and 76.9%,

Table 1 CO hydrogenation performances over different Rh-based catalysts

Cat.	Conv. CO (%)	Selectivity of products (C%)						STY$_{C2\text{-}oxy}$ g/(kg-cat h)
		C_{2+}^{a}	CH_4	EtOH	HAc	HOAc	C$_2$-oxy^{b}	
Rh/Silica	8.1	8.4	20.1	9.7	35.4	18.7	71.2	493.6
Rh/Silica-C$_1$OH	8.6	8.0	19.5	9.4	36.1	20.3	72.3	539.8
Rh/Silica-C$_2$OH	8.8	7.3	18.2	9.1	37.3	20.8	74.3	564.8
Rh/Silica-C$_3$OH	9.3	6.9	17.7	8.3	38.3	21.6	75.4	607.0
Rh/Silica-C$_4$OH	9.6	6.1	17.1	7.7	40.2	22.4	76.9	630.8
Rh/Silica-C$_5$OH	7.1	5.3	16.4	8.1	40.0	23.2	78.1	494.8

Reaction conditions: 553 K, 5.0 Mpa (H_2/CO = 2) and GHSV = 12,500 h^{-1}

[a] C_{2+} designates hydrocarbons other than methane

[b] C$_2$-oxy designates oxygenates such as ethanol, acetaldehyde, acetic acids, methyl acetate, and ethyl acetate etc

respectively. Moreover, with increasing the molecule weight of the n-alcohol employed in the silica pretreatment, the S$_{C2\text{-}oxy}$ increased from 72.3% to 78.1% while the STY$_{C2\text{-}oxy}$ first increased, then reached a maximum of 630.8 g/(kg-cat h), and finally decreased to 494.8 g/(kg-cat h). On the other hand, it was noticed that the selectivities to CH_4 and C_{2+} hydrocarbons decreased continuously from 8.0% and 19.5% down to 5.3 and 16.4% respectively with increasing the molecule weight of the n-alcohol used. Thus, it was clear that pretreatment of the silica supports with nC$_1$–C$_5$ alcohols improved significantly the CO hydrogenation performance of the Rh–Mn–Li/SiO$_2$ catalyst. Moreover, the catalytic properties could be further regulated by changing the number of C-atoms in the alcohol molecule employed.

3.2 Rhodium Dispersion

Figure 1 shows typical TEM photographs of the catalysts Rh/Silica, Rh/Silica-C$_2$OH, Rh/Silica-C$_4$OH, and Rh/Silica-C$_5$OH. It was found that the Rh particles were dispersed with the same spherical shapes on these catalysts, and that the rhodium particle size decreased consecutively from Rh/Silica, Rh/Silica-C$_2$OH, Rh/Silica-C$_4$OH, to Rh/Silica-C$_5$OH catalyst. The average particles sizes obtained by the statistical calculation from all the TEM images for the above catalysts were 3.7, 3.2, 2.8, and 2.5 nm, respectively.

The uptakes of CO and H_2 on these Rh-based catalysts are summarized in Table 2. Both the CO and H_2 uptakes increased in the order of Rh/Silica < Rh/Silica-C$_2$OH < Rh/Silica-C$_4$OH < Rh/Silica-C$_5$OH, though the increase in H_2 uptake was not so obvious as that in CO uptake. On the basis of the results of TEM and CO and H_2 chemisorption, it could be concluded that the pretreatment of the silica supports with nC$_1$–C$_5$ alcohols enhanced the rhodium dispersion on the Rh–Mn–Li/SiO$_2$ catalysts, thereby increasing the number of active sites available for the reactant molecules. Moreover, this effect of support pretreatment became stronger and stronger with increasing molecule weight of the n-alcohol employed.

3.3 The Chemical State of Rhodium

FT-IR spectra of adsorbed CO on these Rh-based catalysts are shown in Fig. 2. The observed CO adsorption bands are all well established in the literature [6]. The broad band centering at ca. 1,820 cm^{-1} is ascribed to the bridge-bonded CO and the band at ca. 2,063 cm^{-1} to linearly adsorbed CO, while the bands at ca. 2,034 and 2,100 cm^{-1} correspond to the geminal CO surface species. As shown in Fig. 2, the intensity of geminal CO significantly increased consecutively from Rh/Silica, Rh/Silica-C$_2$OH, Rh/Silica-C$_4$OH, to Rh/Silica-C$_5$OH catalyst, while that of the linear and bridge-bonded CO changed only a little. It is well established that the bridge-bonded and linear CO are formed on the Rh^0 sites and that the geminal CO is on the Rh$^+$ sites [7, 8]. Thus, it could be deduced from the above results that the ratio of Rh$^+$/Rh^0 sites on the reduced catalysts increased consecutively from Rh/Silica, Rh/Silica-C$_2$OH, Rh/Silica-C$_4$OH, to Rh/Silica-C$_5$OH catalyst.

Some researches have discovered that metallic Rh, i.e. Rh^0, is the active sites for CO dissociation, while partially oxidized Rh, i.e. Rh$^+$, is more favorable active sites for CO insertion to form intermediates of C$_2$-oxygenates [9–11]. As discussed above, the support pretreatment with nC$_1$–C$_5$ alcohols increased the Rh dispersion and the ratio of Rh$^+$/Rh^0 sites, thereby increasing the number of active sites, especially the active sites for CO insertion. According to the well-known C$_2$-oxygenates formation mechanism [12, 13], CO hydrogenation to C$_2$-oxygenates requires an initial CO dissociation to form CH$_x$ species. Subsequently, the reaction could proceed mainly through CH$_x$

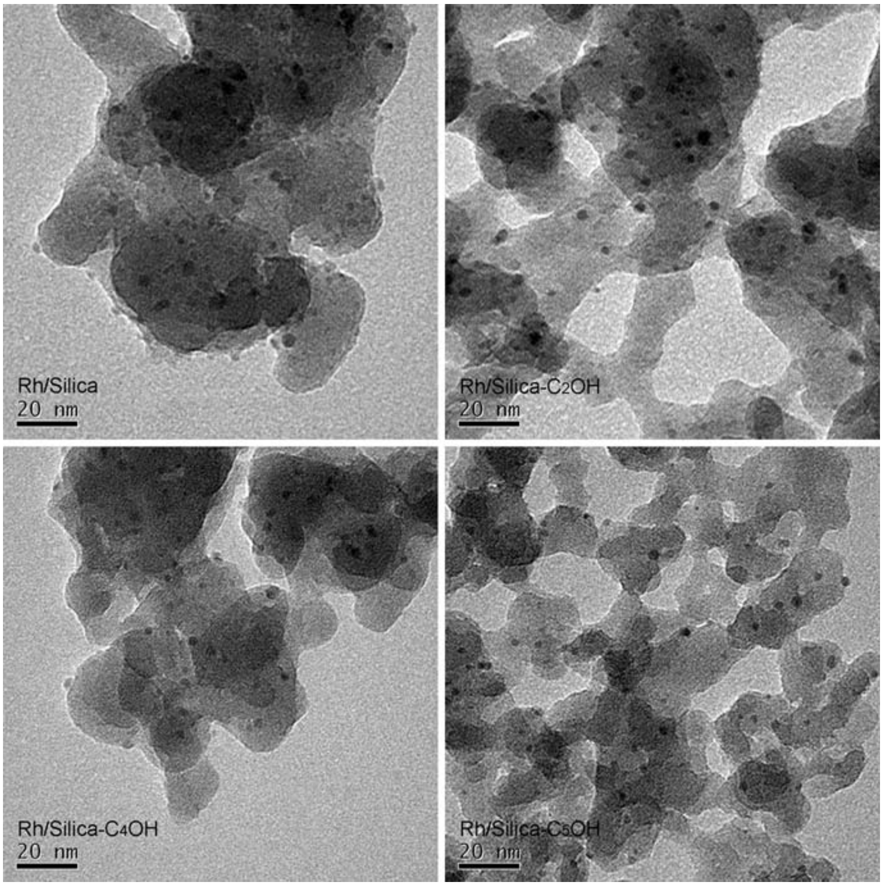

Fig. 1 TEM photographs for different Rh-based catalysts

hydrogenation to produce methane, CO insertion into CH_x followed by H addition to yield C_2-oxygenates, and chain growth through polymerization of CH_x species. Thus, the increase in the number of active sites, especially the active sites for CO insertion, will definitely promoted the formation of C_2-oxygenates from syngas, and accordingly the increasing of $STY_{C2\text{-}oxy}$ and $S_{C2\text{-}oxy}$.

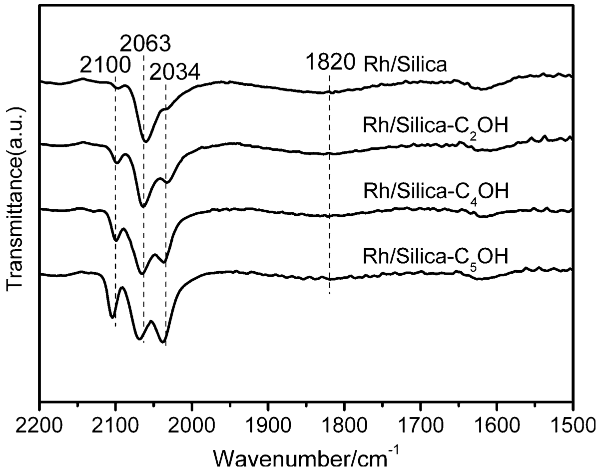

Fig. 2 FT-IR spectra of adsorbed CO on different Rh-based catalysts

Since both Rh^0 and Rh^+ sites are active for CO adsorption, while H_2 is known to adsorb dissociatively on Rh^0 sites [7, 8, 14], the difference in ramping rates of CO and H_2 adsorption (shown in Table 2) could be interpreted by the more obvious increase in Rh^+ sites than that in Rh^0 sites on the reduced catalysts. This difference might imply a consecutive decrease in the relative surface coverage of H* and CO* (θ_H/θ_{CO}) under our reaction conditions from Rh/Silica, Rh/Silica-C_2OH, Rh/Silica-C_4OH, to Rh/Silica-C_5OH catalyst. As a consequence, the hydrogenation rate of adsorbed surface C species to CH_x would decrease from Rh/Silica, Rh/Silica-C_2OH, Rh/Silica-C_4OH, to Rh/Silica-C_5OH catalyst. The decrease in the hydrogenation abilities of the catalysts from Rh/Silica, Rh/Silica-C_2OH, Rh/Silica-C_4OH, to Rh/Silica-C_5OH catalyst was also demonstrated by the increase in the selectivities to acetaldehyde and

Table 2 Uptakes of CO and H_2 on different Rh-based catalysts

	Rh/Silica	Rh/Silica-C_2OH	Rh/Silica-C_4OH	Rh/Silica-C_5OH
CO/Rh	0.32	0.38	0.46	0.52
H/Rh	0.20	0.22	0.24	0.25

acetic acid, and the decrease in the ethanol selectivity according to the above order (shown in Table 1). Since Rh^0 is the active sites for CO dissociation, the relative rate of CO dissociation also decreased according to the above order due to the increasing ratio of Rh^0/Rh$^+$. Thus, the decrease in catalytic activity over the Rh/Silica-C$_5$OH catalyst might be attributed to the excessive decrease in the relative rate of CO dissociation or in the hydrogenation rate of adsorbed surface C species to CH$_x$. In addition, the decrease in the selectivities to CH$_4$ and C$_{2+}$ hydrocarbons with increasing the molecule weight of the n-alcohol employed should be attributed to the decrease in the rate of the CH$_x$ hydrogenation and in the rate of the polymerization of CH$_x$ species, respectively.

3.4 Surface Properties of Silica Support

In an attempt to make clear that how the pretreatment of the silica supports with nC$_1$–C$_5$ alcohols can influence the rhodium dispersion and the chemical state of rhodium, we have investigated the surface properties of the different silica supports by FT-IR. As shown in Fig. 3, the sharp absorption band at 3,743 cm^{-1} is assigned to isolated Si–OH stretching vibrations and the broad band between 3,100 and 3,700 cm^{-1} to the hydrogen-bonded Si–OH stretching vibrations, while the absorption bands at ca. 2,800–3,000 cm^{-1} correspond to C–H stretching vibrations of superficial alkoxyl groups [15–18]. Comparing to the untreated silica support, there is an obvious decrease in the densities of both the isolated Si–OH and the hydrogen-bonded Si–OH on the pretreated silica supports, with the simultaneous appearance of the superficial alkoxyl groups. These results suggest that the alcohol molecules were grafted onto the silica surface by reacting with the Si–OH during the support pretreatment. In addition, there was little difference in the densities of the Si–OH among the pretreated silica supports, which implies that the grafting process was independent of the polarity of the normal alcohol in this study.

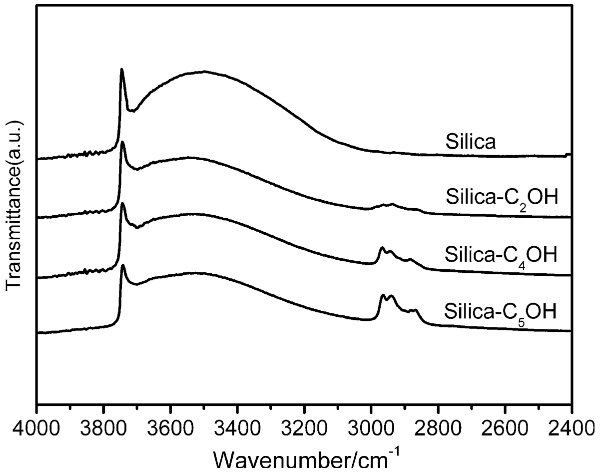

Fig. 3 FT-IR spectra of untreated and pretreated silica supports

Gou et al. [19] have reported that the density of the hydroxyl groups on the silica surface was correlated with the dispersion of the silica-supported metals, and that a higher metal dispersion was achieved with lower Si–OH density. They also proposed the following model to explain the results. At the later stage of the evaporation of water, droplets of the impregnation solution could be formed on the surface of the support. The droplets that were formed on more hydrophobic surfaces would be more easily split or shrunk, resulting in the formation of smaller droplets than those on less hydrophobic surfaces. As a result, the metal precursors may become more highly dispersed on more hydrophobic silica gel. Since the densities of Si–OH decreased and a number of alkoxyl groups formed on the surface of the pretreated silica gels, the silica supports tended to be more hydrophobic. So the above explanation might also be applicable to account for the enhancement of the rhodium dispersion on the catalysts prepared from the pretreated silica supports in this study. Moreover, with increasing molecule weight of n-alcohol employed, the hydrophobicity of the silica surface further increased; hence the rhodium dispersion was correspondingly enhanced. In addition, being hindered from aggregation of the metal precursors by superficial alkoxyl groups during the drying and reduction processes, this might be another important reason for the increase in the rhodium dispersion [4, 18].

According to results reported in the literature [20, 21], promoters such as manganese oxide could act as an electron acceptor and withdraw electrons from the Rh metal, hence resulting in the formation of partially oxidized Rh, i.e., Rh$^+$ sites at the Rh–MnO interface. It was also reported that the existence of manganese species could suppress the reduction of the rhodium precursor, thereby increasing the difficulty of rhodium reduction [22, 23]. Since the rhodium dispersion increased in our work, the rhodium and the promoters such as manganese were expected to contact more extensively. Thus the increase in the ratio of Rh$^+$/Rh^0 sites might be attributed to more extensive interface of rhodium and manganese to be formed due to a better dispersed Rh phase. Further investigations into the surface modification effects of the silica supports with nC$_1$–C$_5$ alcohols for Rh–Mn–Li/SiO$_2$ catalyst are now under way.

4 Conclusion

The CO hydrogenation performance of an Rh–Mn–Li/SiO$_2$ catalyst was significantly improved by pretreating the silica support with $n\text{C}_1$–C_5 alcohols. The improvements in the catalytic properties of the Rh–Mn–Li/SiO_2 catalyst were attributed to the increase in Rh dispersion and in the ratio of Rh^+/Rh^0 sites, i.e., the increase of the number of active sites, especially the active sites for CO insertion. The enhancement in the hydrophobicity of the pretreated silica supports might be responsible for the changes in the Rh dispersion and the chemical state of rhodium.

Acknowledgment This work was financially supported by the National Basic Research Program of China (973 Program) (no. 2005CB221403).

References

1. Chen WM, Ding YJ, Jiang DH, Pan ZD, Luo HY (2005) Catal Lett 104:177
2. Iler RK (1979) The chemistry of silica. Wiley, New York
3. Qu Z, Huang W, Zhou S, Zheng H, Liu X, Chen M, Bao X (2005) J Catal 234:33
4. Ho S, Su Y (1997) J Catal 168:51
5. Zhang Y, Hanayama K, Tsubaki N (2006) Catal Commun 7:251
6. Yang AC, Garland CW (1957) J Phys Chem 61:1504
7. Rice CA, Worley SD, Curtis CW, Guin JA, Tarrer AR (1981) J Chem Phys 74:6487
8. Cavanagh RR, Yates JT (1981) J Chem Phys 74:4150
9. Watson PR, Somorjai GA (1981) J Catal 72:347
10. Chuang SSC, Pien SI (1992) J Catal 135:618
11. Kawai M, Uda M, Ichikawa M (1985) J Phys Chem 89:1654
12. Ichikawa M, Fukushima T (1985) J Chem Soc Chem Commun 6:321
13. Sachtler WMH, Ichikawa M (1986) J Phys Chem 90:4752
14. Nieuwenhuys BE (1983) Surf Sci 126:307
15. Brinker CJ, Sherer GW (1990) Sol-gel science. Academic Press, London
16. Xia QH, Hidajat K, Kawa S (2001) Catal Today 68:255
17. Zimnoch dos Santos JH, Greco PP, Stedile FC, Dupont J (2000) J Mol Catal A Chem 154:113
18. Cortés J, Jimenez R, Araya P (2002) Catal Lett 82:255
19. Guo SL, Arai M, Nishiyama Y (1990) Appl Catal 65:31
20. Wang Y, Song S, Ma D, Luo HY, Liang DB, Bao XH (1999) J Mol Catal A: Chem 149:51
21. Ojeda M, Granados ML, Rojas S, Terreros P, García-García FJ, Fierro JLG (2004) Appl Catal A Gen 261:47
22. Schünemann V, Treviño H, Lei GD, Tomczak DC, Sachtler WMH, Fogash K, Dumesic JA (1995) J Catal 153:144
23. Treviño H, Lei GD, Sachtler WMH (1995) J Catal 154:245